



Paul-Rolf Preußner

## Background: Raytracing?

Raytracing sounds like a modern approach. But this impression is wrong. Raytracing was the first calculation method for imaging optics, developed in the beginning of the seventeenth century. The law of refraction of light at a surface that separates two media of different light velocity was first discovered heuristically by Willebrord Snellius (1580–1626). The numerical value of the light velocity in vacuum  $v_v$  was not yet known at that time, but the ratio of light velocities in different media was. Therefore, the “index of refraction”  $n = v_v / v_m$  was used to optically characterize a specific material with light velocity  $v_m$ . Pierre de Fermat (1601–1665) deduced Snell’s law a few decades after its invention from a general principle of light propagation. This deduction is often presented to students of physics as an exercise: They have to find out the angular change of light propagation on a surface separating two media of different light velocity under the condition that the total flight time of the light has a minimum. The result of this exercise is Snell’s law:  $\sin\beta_1 \times n_1 = \sin\beta_2 \times n_2$  with  $n_1$  and  $n_2$ , refractive indices of the two media, and  $\beta_1$  and  $\beta_2$ , angles of the light ray relative to the normal of the surface at the intersection point.

---

P.-R. Preußner (✉)  
University Eye Hospital Mainz, Mainz, Germany  
e-mail: [pr.preussner@uni-mainz.de](mailto:pr.preussner@uni-mainz.de)

Nothing more than Snell’s law is needed to calculate an imaging optical system, but there is a pitfall: combining expressions of Snell’s law for more than one surface generates so-called transcendental equations which are mathematically not solvable. The only way is to apply Snell’s law iteratively: Calculate the angle of one ray on one surface, use the result for the next surface, and continue this way for all surfaces and for many rays. This needs the calculation of many sine expressions and of the ray geometry between the surfaces for all rays, altogether called “**raytracing**,” requiring a calculation effort that was not available in the seventeenth century. Thus, despite the availability of the physical know how, optical systems could not be calculated at that time.

About 150 years later Carl Friedrich Gauß (1777–1855) found an approximative solution of the problem. Numerically, the sine can be calculated by a polynomial series:  $\sin\beta = \beta - \beta^3 / 3! + \beta^5 / 5! - \beta^7 / 7! \dots$

Gauß abbreviated this series to the first element:  $\sin\beta \approx \beta$ . The accuracy of this approximation is the better the smaller  $\beta$  is. For an optical system consisting of only spherical surfaces and centered to an optical axis, rays with a small angular deviation from this axis could now be calculated in closed formulae, thereby using terms like focal width  $f = R / \Delta n$  or power  $p = 1 / f$  with  $R$ , the radius of the sphere, and  $\Delta n$ , the difference of the refractive indices of both sides of that sphere.

The restriction of Gaussian optics to paraxial rays and to spherical surfaces causes inaccuracies which are not tolerable in many applications. Therefore, the seventeenth-century approach of raytracing has meanwhile again replaced Gaussian optics in nearly all optical areas. The main reason to use Gaussian optics, the missing computing power, disappeared with the availability of cheap, powerful computers today.

Also the human eye with its highly vaulted optical surfaces is poorly described by Gaussian optics. The development of a variety of correcting methods for IOL formulas in Gaussian optics was necessary to compensate the bias from a too simplified approach.

---

## IOL Selection in OKULIX

Tracing many rays through a human eye does not yet solve the problem of finding the IOL that fits best to the patient's requirements. This addresses not only the IOL power closest to the target refraction but also higher order optical errors of the pseudophakic eye, in particular, the eye's spherical aberration, and astigmatism.

Generally, patients want to see "sharp," but, other than in a photograph, the major fraction of the light impinging to the optical entrance of the eye does not contribute to the impression of a subjectively sharp image. The human eye can see sharp only in a very small area, the fovea. Outside the fovea, visual acuity steeply decreases to a few percent of the foveal value. This decrease is mostly caused by the neuronal characteristics of the human retina, less by the decrease of optical imaging quality. Therefore, in order not to waive computing power, OKULIX restricts all calculations to the foveal area.

In the unavoidable presence of higher order optical errors of the human eye, the definition of "sharp" is not always unambiguous. Among other influencing parameters, it can even depend on the visual target. A square-edged target may look sharper than a round one with one optics,

but less sharp with another one. Taking into account this ambiguity together with the requirement to obtain IOL calculation results from raytracing which can directly be compared to those of other methods, the following calculation steps are used in OKULIX:

1. Calculation of the paraxial refraction of the eye for each power level of the corresponding IOL model. The results of such paraxial raytracing are identical to those of a thick-lens calculation in Gaussian optics.
2. Calculation of the so-called best focus refraction in a full aperture raytracing, again for all power levels. The best focus of an optical system with spherical aberration is the focal width of the highest flux density. It is the "working" focus used in vision, and it depends on the pupil width. As an example, the refraction difference between paraxial and the best focus refraction of a mean-sized eye implanted with a 21D Alcon SN60AT IOL is  $-0.2D$  for a pupil width of 2.5 mm, but  $-1.17D$  for 6 mm pupil width. This refraction shift is also responsible for what is commonly called "night myopia." It depends on many parameters, e.g., on the asphericities of all optical surfaces and on the IOL shape factor (see also section "[Impact of IOL Shape Factor Variations](#)").

The default pupil width in OKULIX is 2.5 mm in pupil plane, i.e.,  $\approx 2.9$  mm in corneal plane (modifiable by the user). The best focus refraction can be directly compared to the results of all other IOL calculation methods. The difference between the paraxial and the best focus refraction shows the amount of spherical aberration with the chosen IOL model. It is zero in case of zero spherical aberration.

The best focus refractions are indicated for sphere, cylinder, and axis. Thus the user can see from the axis whether the proposed toric IOL power results in an astigmatic under- or overcorrection, see Fig. 49.1.

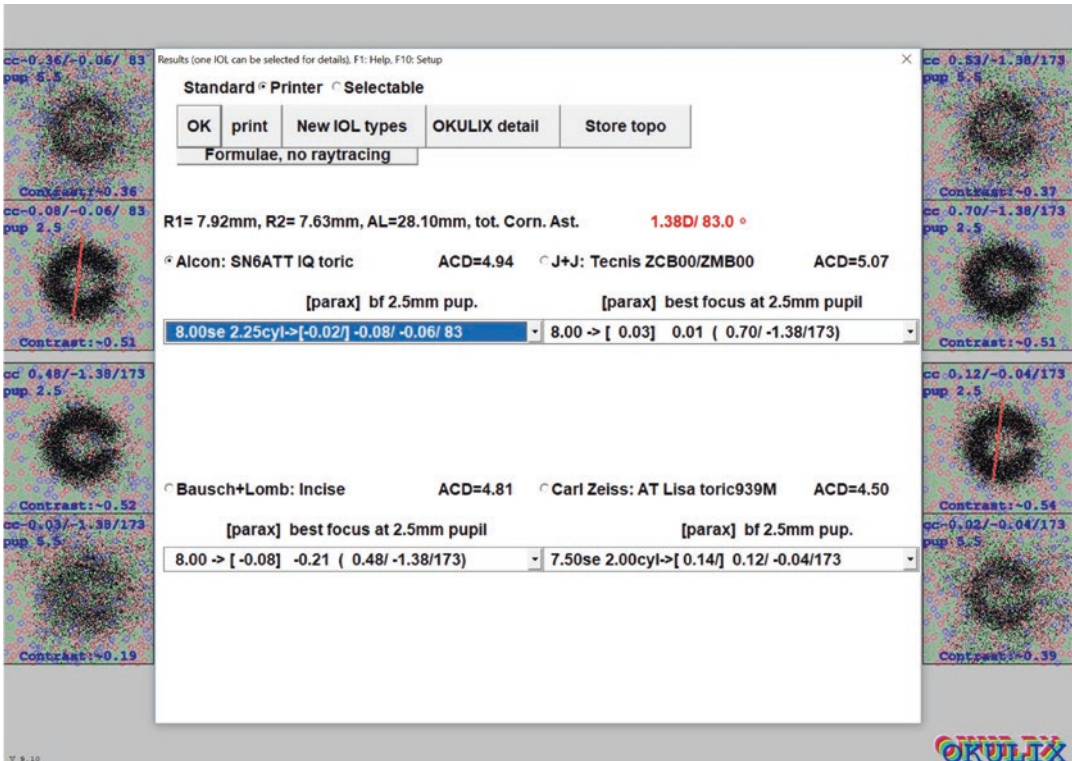


**Fig. 49.1** Results of calculation for four IOL models (The predicted refractions are calculated paraxially and for the best focus of the assumed pupil width (default: 2.5 mm) in pupil plane. They are shown for each power level in the sub-windows of the IOL models. Two Landolt rings of visual acuity chart size 1.0 (20/20, 6/6, logMar 0) are simulated for each IOL model and shown above each other, one with normal (e.g., 2.5 mm) and one with large (5.5 mm) pupil size. The simulations are calculated with

the best sphero-cylindrical correction which is indicated in blue on top of the subimage. Thus the simulated visual impressions exactly show the impact of all higher order optical aberrations. As a quantitative measure of optical quality the contrast of the Landolt rings is indicated (blue). The total corneal astigmatism, i.e., the combination of anterior and posterior astigmatism, is shown in red. The cylinder axis is additionally plotted in the Landolt ring simulations of toric IOL.)

3. Calculation of simulated Landolt ring images on the retina for the IOL power level closest to the target refraction. These images are calculated for 2.5 mm and 5.5 mm pupil width, thus graphically showing the impact of spherical aberration and other higher order optical errors on image quality, see Fig. 49.1. In both images the sphero-cylindrical refraction errors (in corneal plane) are indicated and the calculation is corrected for them. Without such correction, sphero-cylindrical errors mostly would dominate the image worsening compared to the worsening caused by higher order optical errors.

For toric IOL [6, 20], simulated Landolt rings are additionally calculated not only for the power level closest to the target refraction but also for the neighboring spherical and cylindrical power levels, i.e., altogether nine subimages are produced. This time, calculation is performed for 2.5 mm pupil width only (or for the value chosen by the user) and without correction of residual sphero-cylindrical refraction errors, thus showing the patient’s visual impression without glasses, see Fig. 49.2.

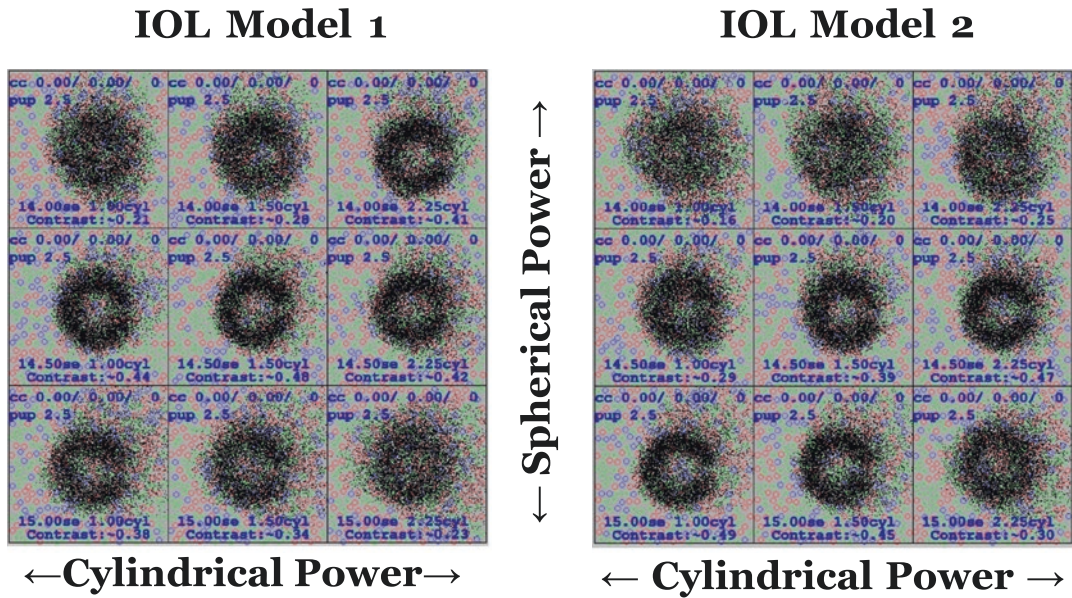


**Fig. 49.2** Step 3 of Toric IOL Selection (The central one of the nine Landolt rings corresponds to the “best focus” selection, and the surrounding ones are from the neighboring power steps in sphere (se) and cylinder. The two IOL models differ in design details, in particular, in the asphericity of their surfaces causing different spherical

aberrations of the eye. Both IOL models are virtually implanted into the same eye. Note that for IOL model 1 the central subimage corresponds to the best visual impression, but for IOL model 2, the lowest left and the middle right are slightly better, showing the ambiguity of “best optics”)

## Input Parameters for IOL Calculation

The accuracy of an IOL calculation is always limited by the accuracy of the input data. Many of the current methods are additionally biased from replacing physical input data by assumed parameters. Even if OKULIX tries to avoid this as far as possible, there are unavoidable restrictions:

1. Data that cannot be measured with the available equipment. Corneal asphericity is not measured when only Keratometry is available, and the data of the posterior corneal surface are only measured with instruments providing full tomography: Scheimpflug or OCT devices. In cases of unavailable measurements, OKULIX uses the eye model of Liou and Brennan [9] to complete the missing input data.

2. Data that cannot be measured at all preoperatively: the final IOL position. OKULIX assumes a centered IOL, and however, after the IOL selection the user can define a decentration and simulate the impact on optical quality, e.g., Landolt ring images or wavefront errors.

OKULIX uses the geometrical IOL position, not a fictitious “effective lens position.” The prediction algorithm of IOL position utilizes axial eye length and position and the thickness of the crystalline lens (when measured) and an average IOL position for each IOL model [17]. During the development of OKULIX, this algorithm was refined several times, thereby taking into account postoperative position measurements of different IOL models [15]. In case of a justified assumption (e.g., measurement in the fellow eye), the user can also define the IOL position in OKULIX. In principal, there is no difference

of such a prediction algorithm used for raytracing compared to the one used for Gaussian optics with respect to accuracy, but an algorithm that predicts “effective” instead of geometrical IOL positions can cause a systematic bias in particular in short eyes.

The measurable input data are described in the following subsections.

## Axial Length Data

Axial lengths measured by different devices differ significantly. Even if the IOLMaster (Zeiss, Germany) is de facto established as a worldwide reference, the rational basis to accept this is doubtful as it is based on a relative calibration of the IOLMaster to an ultrasound device [3], making thus this ultrasound device to the universal standard. However, a real “Gold Standard” for axial length measurements does not exist because it is impossible to measure a human eye, e.g., by a mechanical micrometer. To overcome these problems of absolute calibration, during the development of OKULIX, an axial length transformation was developed that was calibrated in a patient collective in which all other parameters were defined with high accuracy. Corneal radii, axial lengths (from IOLMaster), IOL position (from laser interferometry), and refraction were measured in a patient collective of 189 eyes. Together with these data, manufacturer’s IOL data (see below) were used for a raytracing calculation. The data set of this pseudophakic sample is mathematically overdetermined, and therefore, we could find a transformation for the axial lengths that made the data consistent [11, 12, 15]. The results of this transformation are used as reference in OKULIX. For other axial length measuring devices, comparing measurements was performed to the IOLMaster in larger patient collectives to establish relative calibrations of all of these devices to one another. Thus each of the devices listed in OKULIX can now be used,

together with an internal transformation procedure, without inducing any systematic differences.

The accuracy of axial length measurements is limited by the unknown properties of the crystalline lens which cannot be measured independently from the thickness in the individual eye: the sound velocity in ultrasound and the refractive index in optical measurements. In order to find out the impact of these parameters on overall accuracy, the axial length was optically measured prior to and after cataract surgery in a large patient collective. In the postoperative measurement, the data (thickness and refractive index of the IOL) were exactly known. The standard deviation of the difference between pre- and postoperative measurements (52  $\mu\text{m}$ , [17]) can be considered as the best measure of the mean error.

In summary, with modern optical axial length measurements, errors are in the order of 50  $\mu\text{m}$  corresponding to  $\approx 0.15\text{D}$  in the refraction prediction. This is valid for all IOL calculation methods.

## Corneal Data

Preferably, corneal data should consist of the measured tomography, i.e., anterior topography and spatially resolved thickness. Devices that have a software interface to OKULIX transfer these data automatically. Such devices are Tomey TMS-5 and CASIA, Oculus Pentacam, Ziemer Galilei G6, and Heidelberg Engineering ANTERION. Local posterior corneal radii are calculated from the anterior ones and the local thickness in a straightforward geometrical calculation. Some other devices with an interface to OKULIX only measure anterior topography: Tomey TMS4 and OA2000 and Tracey iTrace. For the latter ones, local posterior radii are calculated according to the Liou and Brennan eye model [9] from the anterior ones:  $R_p = 0.83 \times R_a$  with  $R_p$  and  $R_a$ , local posterior and anterior radii. This calculation should not be performed in eyes after the corneal surgery.

When only keratometric (vertex) radii are measured, they can be used as well for “normal” eyes, again by calculating the posterior vertex radii with the same factor of 0.83 from the anterior ones, and a default value of  $-0.18$  for anterior corneal asphericity. However, in this case, the third step of the IOL selection as described in section “[IOL Selection in OKULIX](#)” does not make much sense.

## IOL Data

An IOL in OKULIX is defined by anterior and posterior vertex radii, central thickness, refractive index, and asphericity of anterior and posterior surfaces. In toric models, two vertex radii are needed for each anterior or posterior toric surface. These data are different for each power level, whereby “power” is only used as a label (rather than as a physical parameter). All IOL data in OKULIX come from the IOL manufacturers. To avoid possible data errors, all data are checked for compliance with ISO11979-2 prior to inclusion into the OKULIX database. The notation of toric IOLs also is in compliance with ISO11979-2, for example, 23.5Se2.5Cyl means an IOL with a spherical equivalent of 23.5D and a cylinder power of 2.5D. The meridian of the lowest IOL power which is to be implanted at the axis of highest total corneal power is always indicated by a red line.

## Benefits: Applications and Comparisons

### IOL Calculation in Eyes After Corneal Surgery

Two significant differences between virgin eyes and eyes after the corneal surgery can cause errors in the IOL calculation:

1. The asphericity of the anterior cornea often changes from a slightly prolate to an oblate asphere after the myopia-correcting corneal surgery. Keratometric measurements assum-

ing a sphere or a prolate asphere then underestimate the vertex radius [13, 14, 16], thus producing a hyperopic outcome of IOL calculations.

2. With changed anterior but more or less unchanged posterior corneal radii after corneal surgery, the ratio between anterior and posterior corneal radii changes as well. When anterior and posterior surfaces are combined to only one surface at the location of the anterior cornea in IOL formulas, thereby defining a so-called fictitious corneal refractive index  $\hat{n} = n_c + (n_h - n_c) \cdot R_a / R_p - d \cdot (n_c - 1) \cdot (n_h - n_c) / (n_c \cdot R_p)$  with  $n_c$  and  $n_h$ , refractive index of cornea and aqueous humor,  $R_a$  and  $R_p$ , anterior and posterior corneal radii, and  $d$ , corneal thickness, this refractive index  $\hat{n}$  and the corneal power-based thereon are changing as well. After the myopia-correcting corneal surgery, this additionally causes a hyperopic shift.

The said errors do not occur in tomography-based raytracing [2, 21, 23] because all parameters are measured, without making any assumptions, see the following example: In 70 eyes after the myopia-correcting Lasik, Pentacam tomography and IOLMaster Keratometry and axial length measurements were performed prior to the complication-free cataract surgery. Figure 49.3 shows the results together with the impact of the two abovementioned error contributions. In this example, they are both of the

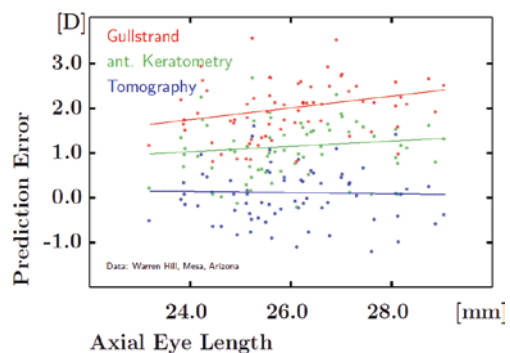


**Fig. 49.3** Prediction error in Post-Lasik eyes blue: raytracing based on full tomography green: same posterior radii, but anterior keratometry (IOLMaster) red: anterior keratometry, posterior radii from Gullstrand’s eye model

same order of magnitude, but this can differ depending on the details of the Lasik laser protocol.

A more systematic approach of verifying whether the impact of a corneal laser surgery is fully covered by an IOL calculation method is the following: The eyes are measured prior to and after the corneal surgery, and for both measurements, an IOL calculation with the same IOL model and power is performed. The differences of the resulting refractive predictions of the IOL calculations should be identical to the achieved corneal laser refractive corrections. The advantage of this approach is to avoid any error impact of the surgical procedure or of IOL manufacturing errors.

Such an investigation was performed in 204 eyes undergoing SMILE. Pre- and postoperative Pentacam tomography and IOLMaster axial length measurements were performed [8]. The OKULIX results together with those of two other methods using Pentacam anterior vertex radii are shown in Fig. 49.4.

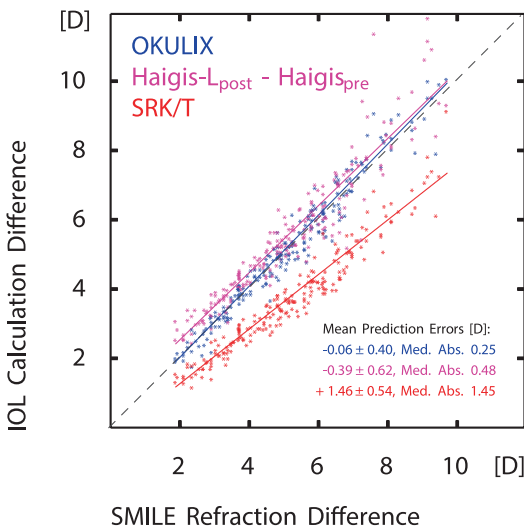


**Fig. 49.4** Prediction errors after SMILE (The difference between the refraction prediction of IOL calculation methods prior to and after the SMILE corneal surgery is shown as a function of the achieved refractive correction of the SMILE procedure in 204 eyes)

## Very Long Eyes

In very long eyes many IOL formulas produce a hyperopic bias which is not found with OKULIX, see Fig. 49.5. The reason, however, is not the application of raytracing but the use of the appropriate eye model of Liou and Brennan [9]. Replacing the fictitious corneal refractive index  $\hat{n}$  of the formulas by the one derived from the Liou and Brennan eye model mostly removes the bias [18, 19]. The wrongly higher  $\hat{n}$ -value from Gullstrand's eye model is also responsible for the unrealistically high "effective lens position" to compensate the overestimated corneal power in the formulas. This applies also to short eyes.

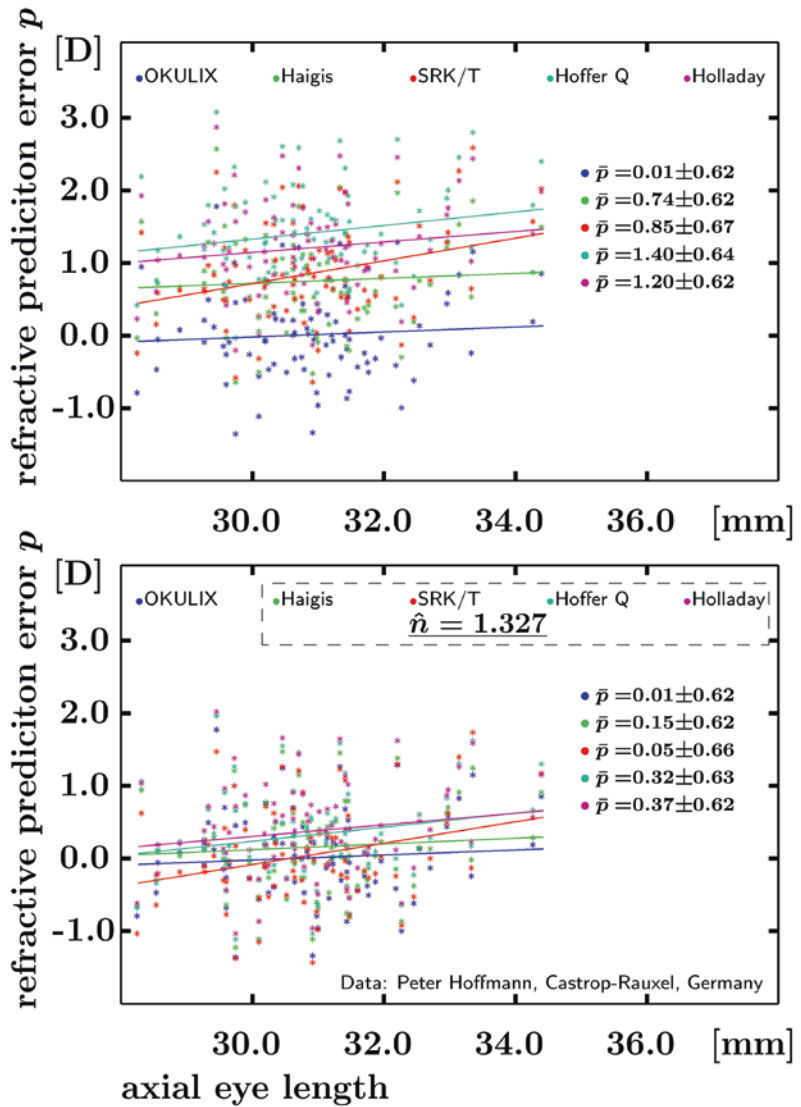
## Impact of IOL Shape Factor Variations

When prediction accuracy was compared to other methods up to the second digit behind the decimal point in a competition, OKULIX was the winner [1]. This, however, is not fully obvious when taking into account the expected error amounts as described in section "Limitations". It can be assumed that the reason is the exact use of the IOL manufacturer's data, in particular, variations of the IOL shape factor with the IOL power level.

The shape factor  $S$  of a lens describes the deviation from biconvex or biconcave symmetry:  $S = (R_1 + R_2) / (R_1 - R_2)$  with  $R_1$  and  $R_2$ , anterior and posterior lens radii. For a symmetric lens,  $R_1 = -R_2$  and thus  $S = 0$ . Many IOL models are symmetric, but the majority of lenses on the market are not. In many of these asymmetric lenses, the shape factor varies between power levels, see Fig. 49.6.

Such shape factor variations also show the occurring inaccuracies when so-called formula constants are adjusted: A correct adjustment would need a separate "constant" for each power level.

**Fig. 49.5** Prediction error in very long eyes (The prediction error of 83 eyes measured with IOLMaster (Zeiss) and implanted with Alcon MA60MA IOLs is shown as a function of the axial eye length. Upper image: results of the formulas [3, 4, 7, 22] in the original notation, and lower image: with Liou and Brennan’s fictitious corneal refractive index)



**Comparison with the “Big Data” Approach**

Systematic deviation patterns of IOL formula predictions from reality can be detected in large collectives implanted with the same IOL model. Moreover, known results from collectives covering the whole range of all input variables can also be used for IOL selections. Such Big Data algorithms do not even need any optical calculation

but can predict IOL powers for individual eyes by higher order inter- or extrapolation from the existing refractive outcome of previous IOL implantations. The Hill RBF method uses radial basis functions (RBFs) for such calculations. In a private communication with Warren Hill, Mesa, Arizona, a set of 6004 eyes implanted with Alcon SN60WF IOL was investigated. The refractive prediction differences between four classical formulas in Gaussian optics [3, 4, 7, 22], the RBF



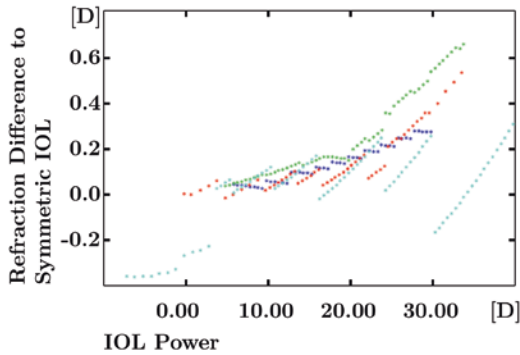


**Fig. 49.6** Shape factor variations (For four different IOL models from four manufacturers (four colors), the differences of the predicted refractions between their IOL and a symmetric IOL (shape factor = 0) of the same power, thickness, and refractive index at the same position in the same eye are shown as a function of the IOL power)

method, and OKULIX were calculated. Differences between each of the formulas and OKULIX show a specific pattern, depending on the assumptions (e.g., fictitious corneal refractive index and effective lens position) of the respective formula. Interestingly, these patterns are principally the same for the differences between the formulas and OKULIX on the one hand and for the differences between the formulas and RBF on the other hand, beside some higher noise for RBF, see Fig. 49.7 in which the results of the comparison for the SRK/T- and for the Haigis formula are shown as examples. A systematic difference pattern between RBF and OKULIX is not recognizable. Correspondingly, only mar-

ginal differences were found in the overall accuracy comparison between RBF and OKULIX (e.g., numbers of eyes within a certain prediction error interval, etc.). However, slightly higher prediction accuracy was found for RBF and for OKULIX when compared to the formulas.

The similar results of RBF and OKULIX do not imply that a Big Data approach is equivalent to a raytracing calculation. A Big Data method needs large numbers of previous IOL implantations for each IOL model separately because of the different IOL shape factor patterns of different IOL models (see section “[Impact of IOL Shape Factor Variations](#)”). Additionally, in eyes after corneal refractive surgery, a large patient collective would not only be needed for each IOL model but also for the combination of an IOL model and a specific protocol of the corneal laser procedure. This is not feasible. In addition, a Big Data approach would not adequately address rare specific characteristics of an individual eye, e.g., a beginning Keratoconus, which would always be detected by corneal tomography and adequately addressed by a raytracing calculation based thereon. Furthermore, the Big Data approach is restricted to spherical equivalents and cannot predict toric IOL with the same algorithms. Finally, the data set of a Big Data approach is based on data collections from many different locations. The accuracy of these subcollectives is often biased by different refraction habits, see also section “[Accuracy of Refraction](#)”.

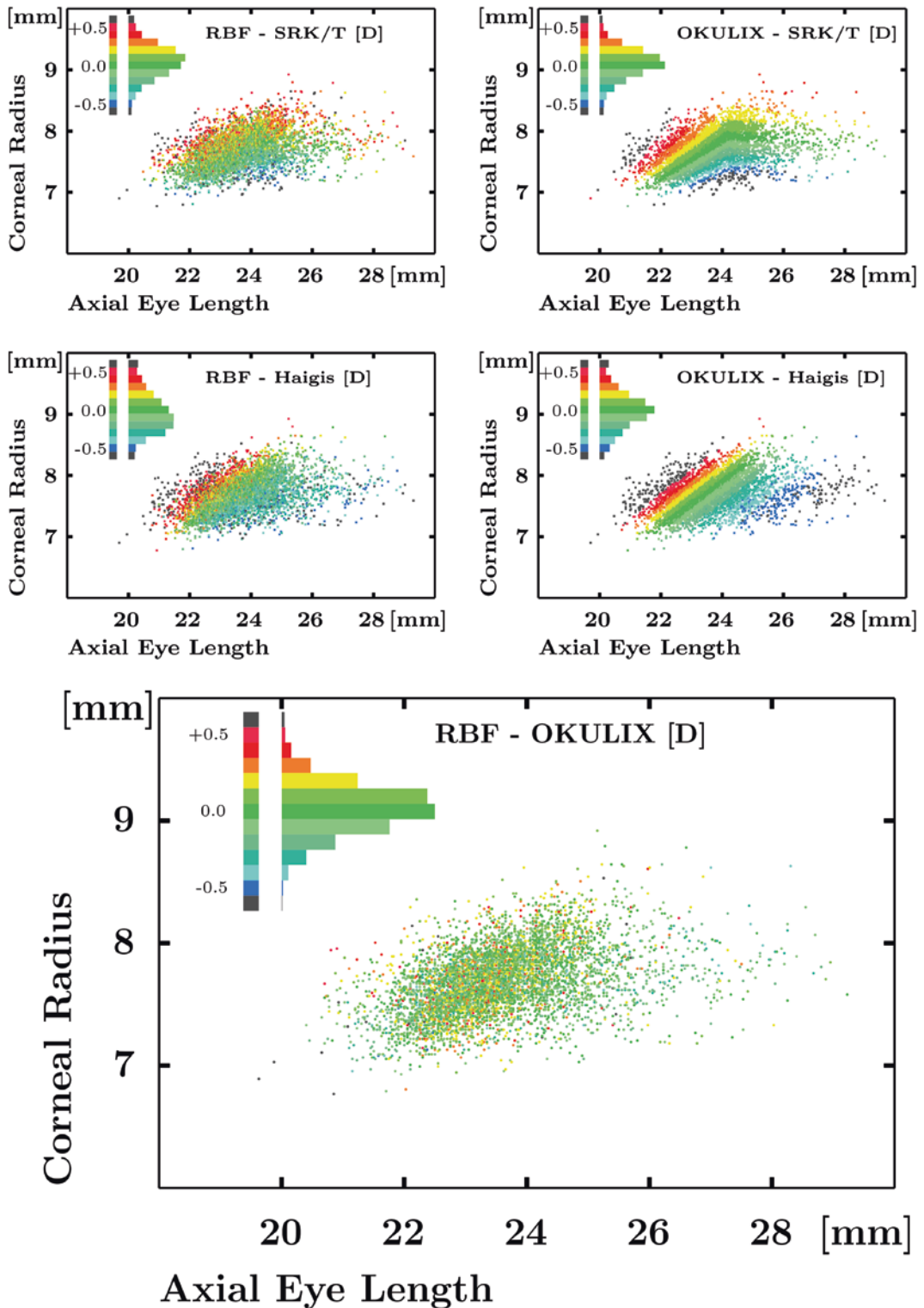


**Fig. 49.7** Systematic differences in 6004 eyes (All subimages show the prediction differences (spherical equivalent) of the indicated methods in pseudocolors, as function of axial eye length and mean corneal radius. The pseudocolor definitions (look-up tables) and the histo-

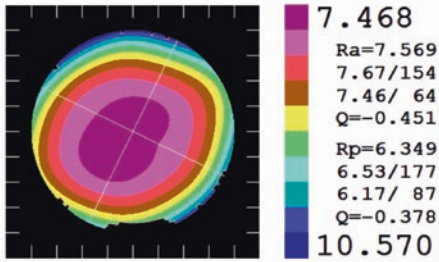
gram distributions of the differences are shown in the upper left corners. Differences of more than  $\pm 0.5D$  are indicated in black. Such higher differences are mostly found in the margins of the distribution in the comparisons with the formulas)

### Additional Tools

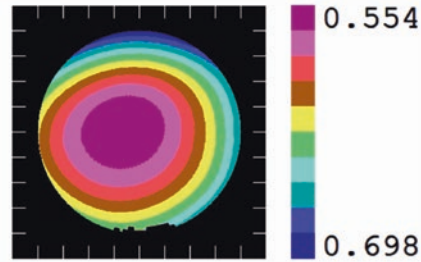
For scientific purposes beyond IOL selection, the corneal module of OKULIX allows additional investigations of the optical properties of the

pseudophakic eye. Two-dimensional refraction- or wavefront maps can be calculated and decomposed into Zernike series up to 12th radial order, see Fig. 49.8 for an example.

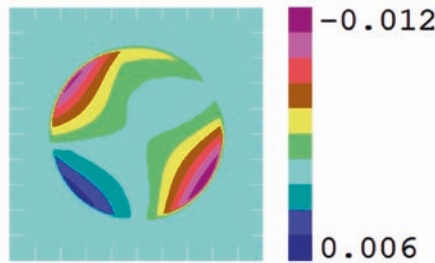
#### Local Corneal Radii



#### Local Corneal Thickness

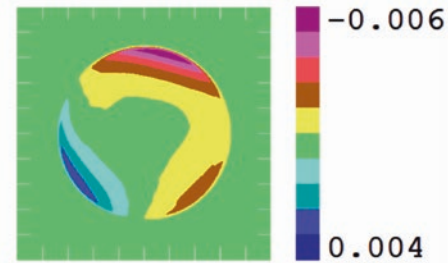


#### Wavefront with spheric IOL



RMS (r<3.0mm) : 0.00270

#### Wavefront with toric IOL



RMS (r<3.0mm) : 0.00100

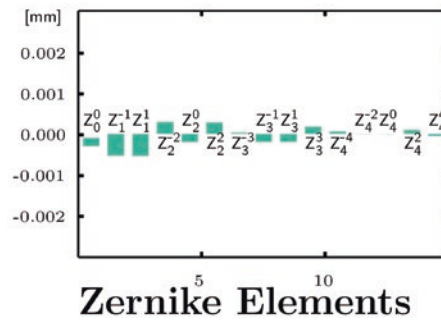
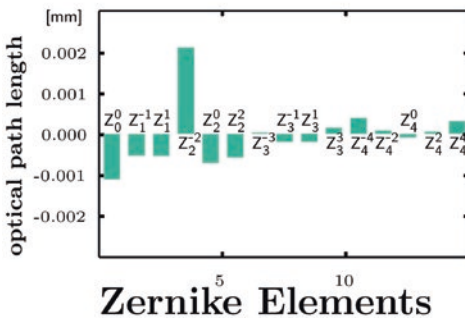


**Fig. 49.8** Wavefront analysis with different IOL models (For an eye with an axial length of 25.28 mm and tomography as shown on top, a wavefront analysis is performed with a spheric (left) and a toric (right) IOL. Both IOL models also differ in the asphericities of their surfaces. The root-mean-square error of optical path lengths inside

a zone of radius 3 mm is about three times as high for the left compared to the right IOL (0.0027 mm versus 0.001 mm). The first 15 Zernike elements out of the overall 91 are shown on the bottom for both IOL models. All not indicated measures are in millimeters)

## Limitations

### Accuracy of Refraction

The accuracy of IOL calculations is mostly measured by the prediction error, i.e., the difference between achieved and predicted refraction. But also these achieved refractions are often not well defined. Refraction errors increase with decreasing visual acuity because patients cannot distinguish between different optical situations, the less, the worse their visual acuity, and the higher their pseudoaccommodation width is. In a patient collective of 115 eyes implanted with aberration correcting IOL and visual acuity of 20/20 or better, the mean absolute prediction error was 0.21D, and in 210 eyes implanted with spherical IOL and visual acuity below 20/20, it was two times as high: 0.42D. All eyes were operated complication free by the same surgeon [5].

In addition to such patient-based error sources, also refraction habits can have a significant impact on the results and can be responsible for the major part of differences between different locations which later are to be compensated by so-called constant optimization of IOL calculations.

### Accuracy of Placido/Scheimpflug Tomographers

In 83 eyes the measured data of three Placido and Scheimpflug tomographers were compared: Galilei G6, a combined Placido- and Scheimpflug tomographer (Ziemer, Switzerland), Pentacam HR, a pure Scheimpflug device (Oculus, Germany), and TMS-5, again a combined Placido–Scheimpflug device (Tomey, Japan). The recorded data of anterior topography and spatially resolved corneal thickness were transferred to OKULIX, and an IOL calculation was performed for the same IOL in the same position and the same axial length. For each eye the predicted refractions were calculated, together with the mean of the three devices and the differences of the individual values to this mean, see Fig. 49.9

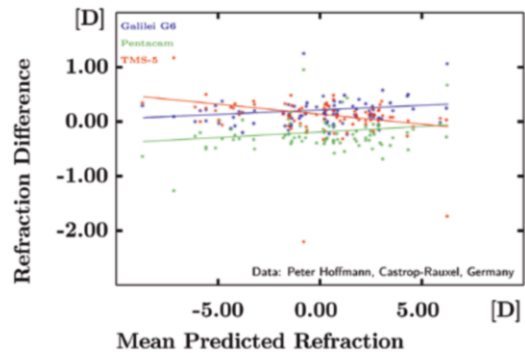


**Fig. 49.9** Differences between Placido and Scheimpflug devices (Assuming an IOL (Johnson and Johnson, Sensor AR40e, 21D) at a position of 4.0 mm behind the cornea and an axial length of 23.6 mm, the residual refractions and the differences between the three devices are calculated. The average differences are  $0.17 \pm 0.24$ D (Galilei G6),  $-0.26 \pm 0.29$  (Pentacam), and  $0.08 \pm 0.39$  (TMS-5))

In addition, the total corneal astigmatism was calculated in OKULIX. For each eye the vector mean of the astigmatisms of the three devices and the vector differences between this mean and the data from each device were determined. The centroids of these differences, describing the systematic deviations, are  $0.04\text{D}/173^\circ$  (Galilei G6),  $0.14\text{D}/93^\circ$  (Pentacam), and  $0.10\text{D}/7^\circ$  (TMS-5). The median absolute values of the astigmatic differences are 0.31D for Galilei G6, 0.33D for Pentacam, and 0.29D for TMS-5.

In summary, the astigmatic differences are small enough to make the three devices exchangeable with respect to the astigmatic error of toric IOL calculations. The spherical differences, however, are just at the limit of acceptability.

### Accuracy of OCT Tomographers

In 161 eyes the measured data of three OCT tomographers were compared: ANTERION (Heidelberg Engineering, Germany), CASIA (Tomey, Japan), and IOLMaster700 (Zeiss, Germany). The recorded data of anterior topography and spatially resolved corneal thickness of ANTERION and CASIA were transferred to OKULIX. From these data, anterior and posterior corneal vertex radii and asphericities were

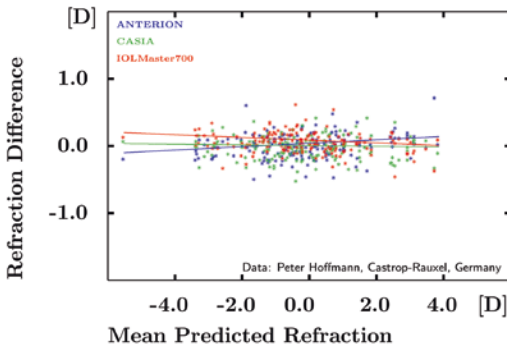


**Fig. 49.10** Differences between OCT devices (Assuming the IOL (Johnson and Johnson, Sensar AR40e, 21D) at a position of 4.0 mm behind the cornea and an axial length of 23.6 mm, the average refractions and the differences between the three devices are calculated. The average differences are  $0.01 \pm 0.21D$  (ANTERION),  $-0.03 \pm 0.21$  (CASIA), and  $0.02 \pm 0.20$  (IOLMaster700))

extracted. For IOLMaster700, anterior and posterior corneal vertex radii were taken from the device because it does not have a software interface to OKULIX. Anterior asphericity was set to  $-0.18$  for the IOLMaster data. An IOL calculation was performed for the same IOL at the same position and the same axial length. For each eye the predicted refractions were calculated, together with the mean of the three devices and the differences of the individual values to this mean, see Fig. 49.10.

In addition the total corneal astigmatism was calculated in OKULIX. For each eye the vector mean of the astigmatisms of the three devices and the vector differences between this mean and the data from each device were determined. The centroids of these differences, describing the systematic deviations, are  $0.18D/120^\circ$  (ANTERION),  $0.07D/70^\circ$  (CASIA), and  $0.22D/4^\circ$  (IOLMaster700). The median absolute values of the astigmatic differences are  $0.26D$  for ANTERION,  $0.30D$  for CASIA, and  $0.33D$  for IOLMaster700.

In summary, the differences between the data of these devices are sufficiently small to make the devices interchangeable with respect to the accuracy of spherical and of toric IOL calculation.

## IOL Manufacturing Tolerances

The IOL manufacturing tolerances for an IOL of power  $P$  according to ISO11979-2 are  $\pm 0.3D$  for  $|P| < 15D$ ,  $\pm 0.4D$  for  $15D \leq P < 25D$ ,  $\pm 0.5D$  for  $25D \leq P < 30D$ , and  $\pm 1.0D$  for  $P \geq 30D$ . Even if many IOL manufacturers claim to produce their IOL with significantly smaller tolerances, it can be assumed that often a major part of systematic power bias of an IOL model is due to an offset in the manufacturing control procedure. OKULIX therefore allows an offset correction of the IOL power of each model which is ultimately comparable to the so-called constant optimizations of IOL formulas.

## Conclusions and Future Developments

IOL calculation with OKULIX raytracing can be performed in the same way and with principally the same accuracy in very long eyes, very short eyes [10, 24], postrefractive eyes, and virgin eyes without any knowledge about the eye's history. This advantage on the one hand requires full confidence in the measured data on the other hand, particularly, in corneal tomography. In addition, also reliable measurements of position and the thickness of the crystalline lens are needed for a sufficiently accurate prediction of the IOL position. These requirements on instrumentation are currently not yet generally fulfilled. However, improvements in instrument development and better availability of such reliable instrumentation are to be expected in the near future.

## References

1. Cooke DL, Cooke TL. A comparison of two methods to calculate axial length. *J Cataract Refract Surg.* 2019;45:284–91.
2. Gjerdrum B, Gundersen KG, Lundmark PO, Aakre BM. Refractive precision of ray tracing IOL calculations based on OCT data versus traditional IOL cal-

- calculation formulas based on reflectometry in patients with a history of laser vision correction for myopia. *Clin Ophthalmol.* 2021;15:845–57.
3. Haigis W, Lege B, Miller N, Schneider B. Comparison of immersion ultrasound biometry and partial coherence interferometry for intraocular lens calculation according to Haigis. *Graefes Arch Clin Exp Ophthalmol.* 2000;238:765–73.
  4. Hoffer KJ. The Hoffer Q formula: a comparison of theoretic and regression formulas. *J Cataract Refract Surg.* 1993;19(11):700–12. Errata: 1994;20(6):677 and 2007;33(1):2–3.
  5. Hoffmann P, Wahl J, Preußner PR. Accuracy of intraocular lens calculation with raytracing. *J Refract Surg.* 2012;28:650–5.
  6. Hoffmann P, Wahl J, Hütz W, Preußner PR. A ray tracing approach to calculate toric intraocular lenses. *J Refract Surg.* 2013;29:402–8.
  7. Holladay JT, Musgrave KH, Prager CT, Lewis JW, Chandler TY, Ruiz RS. A three-part system for refining intraocular lens power calculations. *J Cataract Refract Surg.* 1988;14:17–24.
  8. Lazaridis A, Schraml F, Preußner PR, Sekundo W. Predictability of intraocular lens calculation after SMILE for myopia. *J Cataract Refract Surg.* 2021;47:304–10.
  9. Liou HL, Brennan NA. Anatomically accurate, finite model eye for optical modeling. *J Opt Soc Am.* 1997;14:1684–95.
  10. Luo Y, Li H, Gao L, Du J, Chen W, Gao Y, Ye Z, Li Z. Comparing the accuracy of new intraocular lens power calculation formulae in short eyes after cataract surgery: a systematic review and meta-analysis. *Int Ophthalmol.* 2022. <https://doi.org/10.1007/s10792-021-02191-4>.
  11. Preußner PR, Wahl J, Lahdo H, Findl O. Konsistente IOL-Berechnung. *Ophthalmologe.* 2000;3:300–4.
  12. Preußner PR, Wahl J, Lahdo H, Findl O, Dick B. Ray tracing for IOL calculation. *J Cataract Refract Surg.* 2002;28:1412–9.
  13. Preußner PR, Wahl J, Kramann C. Corneal model. *J Cataract Refract Surg.* 2003;29:471–7.
  14. Preußner PR, Wahl J. Simplified mathematics for customized refractive surgery. *J Cataract Refract Surg.* 2003;29:462–70.
  15. Preußner PR, Wahl J, Weitzel D, Berthold S, Kriechbaum K, Findl O. Predicting postoperative anterior chamber depth and refraction. *J Cataract Refract Surg.* 2004;30:2077–83.
  16. Preußner PR, Wahl J, Weitzel. Topography based IOL power selection. *J Cataract Refract Surg.* 2005;31:525–33.
  17. Preußner PR, Olsen T, Hoffmann P, Findl O. IOL calculation accuracy limits in normal eyes. *J Cataract Refract Surg.* 2008;34:802–8.
  18. Preußner PR, Hoffmann P, Petermeier K. Vergleich zwischen Raytracing und IOL-Formeln der 3. Generation. *Klin Monatsbl Augenheilk.* 2009;226:83–9.
  19. Preußner PR. Intraocular lens calculation in extreme myopia. *J Cataract Refract Surg.* 2010;36:531–2.
  20. Preußner PR, Hoffmann P, Wahl J. Impact of posterior corneal surface on toric intraocular lens (IOL) calculation. *Curr Eye Res.* 2015;40:809–14.
  21. Rabsilber TM, Reuland AJ, Holzer MP, Auffarth GU. Intraocular lens power calculation using ray tracing following excimer laser surgery. *Eye.* 2007;21:697–701.
  22. Retzlaff JA, Sanders DR, Kraff MC. Development of the SRK/T intraocular lens power calculation formula. *J Cataract Refract Surg.* 1990;16:333–40. Errata: 1990;16:528 and 1993;19(5):444–446
  23. Savini G, Hoffer KJ, Schiano-Lomoriello D, Barboni P. Intraocular lens power calculation using Placido disk-Scheimpflug tomographer in eyes that had previous myopic corneal excimer laser surgery. *J Cataract Refract Surg.* 2018;44:935–41.
  24. Wendelstein J, Hoffmann P, Hirschschall N, Fischinger IR, Mariacher S, Wingert T, Langenbacher A, Bolz M. Project hyperopic power prediction: accuracy of 13 different concepts for intraocular lens calculation in short eyes. *Br J Ophthalmol.* 2020. <https://doi.org/10.1136/bjophthalmol-2020-318272>.

**Open Access** This chapter is licensed under the terms of the Creative Commons Attribution 4.0 International License (<http://creativecommons.org/licenses/by/4.0/>), which permits use, sharing, adaptation, distribution and reproduction in any medium or format, as long as you give appropriate credit to the original author(s) and the source, provide a link to the Creative Commons license and indicate if changes were made.

The images or other third party material in this chapter are included in the chapter's Creative Commons license, unless indicated otherwise in a credit line to the material. If material is not included in the chapter's Creative Commons license and your intended use is not permitted by statutory regulation or exceeds the permitted use, you will need to obtain permission directly from the copyright holder.

